

A Search for Very Low-mass Stars and Brown Dwarfs in the Young σ Orionis cluster

V. J. S. Béjar, M. R. Zapatero Osorio, R. Rebolo

Instituto de Astrofísica de Canarias, E-38200 La Laguna, Tenerife. Spain

e-mail addresses: vbejar@ll.iac.es, mosorio@ll.iac.es, rrl@ll.iac.es

Received _____; accepted _____

Accepted for publication in ApJ Main Journal

ABSTRACT

We present a CCD-based photometric survey covering 870 arcmin² in a young stellar cluster around the young multiple star σ Orionis. Our survey limiting R , I , and Z magnitudes are 23.2, 21.8, and 21.0, respectively, with the completeness being about 2.2 mag brighter. From our colour-magnitude diagrams, we have selected 49 faint objects ($I = 15$ –21 mag), which smoothly extrapolate the photometric sequence defined by more massive known members. Adopting the currently accepted age interval of 2–10 Myr for the Orion 1b association, in which σ Orionis is located, and considering recent evolutionary models, our objects may span a mass range from 0.1 down to $0.02 M_{\odot}$, well within the substellar regime.

Follow-up low-resolution optical spectroscopy (635–920 nm) for eight of our candidates in the magnitude range $I = 16$ –19.5 shows that they have spectral types M6–M8.5 which are consistent with the expectations for true members. Compared with their Pleiades counterparts of similar types, H α emission is generally stronger, while Na I and K I absorption lines appear weaker, as expected for lower surface gravities and younger ages. Additionally, TiO bands and in particular VO bands appear clearly enhanced in our candidate with the latest spectral type, SOri 45 (M8.5, $I = 19.5$), compared to objects of similar types in older clusters and the field. We have estimated the mass of this candidate at only 0.020 – $0.040 M_{\odot}$, hence it is one of the least massive brown dwarfs yet discovered.

We examine the potential role of deuterium as a tracer of both substellar nature and age in very young clusters. The luminosity and mass at which the burning/preservation of deuterium takes place is a sensitive function of age and it can therefore provide a determination of the age of a cluster. The σ Orionis

cluster is an excellent site for determining this transition zone empirically, where the most massive brown dwarfs identified are expected to have burned their deuterium content, while the lowest mass ones should have preserved it.

Subject headings: open clusters and associations: individual (σ Orionis) — stars: low-mass, brown dwarfs — stars: evolution — stars: pre-main sequence — stars: fundamental parameters

1. Introduction

Stellar clusters and associations offer a unique opportunity to study substellar objects in a context of known age, distance and metallicity; they are laboratories of key importance in understanding the evolution of brown dwarfs. Deep imaging surveys have revealed a large population of substellar objects in the Pleiades cluster (Rebolo, Zapatero Osorio & Martín 1995; Cossburn et al. 1997; Zapatero Osorio, Rebolo & Martín 1997a; Zapatero Osorio et al. 1997b; Bouvier et al. 1998), demonstrating that the formation of brown dwarfs extends down to masses of $0.035 M_{\odot}$ (Martín et al. 1998a; see also Luhman, Liebert & Rieke 1997). The extension of these studies to other clusters, especially in the younger regions where we can reach objects with lower masses, is therefore very important for confirming and enlarging these results.

The Orion complex is recognized as one of the best sites for understanding star formation processes. Our knowledge of the young, low-mass stellar population in this star forming region has been enriched in recent years with the application of new search techniques for low-mass stars as, for example, $H\alpha$ surveys (Wiramihardja et al. 1989, 1991, 1993; Kogure et al. 1989), and the optical identification of X-ray sources, which were detected by the *ROSAT* all-sky survey (RASS). These recent surveys provided a spatially unbiased sample of X-ray sources over the entire Orion complex (Sterzik et al. 1995; Alcalá, Chavarría-K., & Terranegra 1998; Alcalá et al. 1996). *ROSAT* pointed observations performed on Orion’s Belt (Walter et al. 1994) led to the discovery of a high concentration of X-ray sources near the bright O9.5V star σ Orionis. This star belongs to the Orion 1b association, for which an age of 1.7–7 Myr and a distance modulus of 7.8–8 are estimated (Blaauw 1964; Warren & Hesser 1978, hereafter WH; Brown, de Geus & de Zeeuw 1994, hereafter BGZ). Follow-up photometry and spectroscopy (Wolk 1996) of these X-ray sources have revealed a population of low-mass stars defining a photometric sequence

consistent with the existence of a very young cluster at an age of few million years. This cluster is ideally suited for the detection of very low-mass brown dwarfs and subsequently for investigating the initial mass function in the substellar regime. Additionally, the multiple star σ Orionis is affected by an extinction of $E(B - V) = 0.05$ mag (Lee 1968), and thus, the associated cluster may exhibit very little reddening. At these early ages brown dwarfs are intrinsically more luminous (Burrows et al. 1997; D’Antona & Mazzitelli 1994), which makes their detection and study easier. For example, a $0.025 M_{\odot}$ object is about 7 mag brighter in the absolute magnitude M_I at the age of 5 Myr than at that of the Pleiades cluster (120 Myr) according to the recent tracks of Baraffe et al. (1998). In this paper we present the results of a deep photometric survey of the young cluster around the σ Orionis star in search of its substellar population. We also present follow-up low-resolution spectroscopy of some of our photometric candidates; and we discuss the possibility of using deuterium in studying very young substellar populations.

2. Observations

2.1. Photometry

We have obtained *RIZ* images with the Wide Field Camera (WFC), mounted at the prime focus of the Isaac Newton Telescope (INT), at Observatorio del Roque de los Muchachos (ORM) on the island of La Palma, on 1997 November 29. The camera consists of a mosaic of four 2048×2048 pixel² Loral CCD detectors, providing a pixel projection of 0.37 arcsec. At the time of our observations, one of the CCDs was not in operation, so the effective area of one single mosaic was 478 arcmin². We observed two different regions in each of the three filters, covering a total area of 870 arcmin². Figure 1 shows the location of the two mosaic fields (six CCDs) surveyed. Exposure times were 1200 s for all three filters for the east region and 2×1200 s for the west region.

Raw frames were reduced within the IRAF¹ environment, using the CCDRED package. Images were bias-subtracted and flat-fielded. Due to poor weather conditions at dusk and dawn, it was not possible to take good sky flats. We combined our long-exposure scientific images to obtain the flat-fields we finally used. The photometric analysis was performed using routines within DAOPHOT, which include the selection of stars using the DAOFIND routine (extended objects were mostly avoided) and aperture and psf photometry. Observations at the INT were affected by cirrus; therefore no photometric standard stars were observed at this stage. Average seeing ranged from 1.3 to 2.0 arcsec. In order to transform our INT instrumental magnitudes into the Cousins RI system, we made use of objects in common with images of our fields taken under photometric conditions with the IAC80 Telescope (Teide Observatory on the island of Tenerife) in 1998 January. The IAC80 images were calibrated with standards of Landolt (1992). We estimate the 1σ error in our calibration to be around 0.1 mag. Due to variability in weather conditions at the INT and to the different sensitivity among the CCDs of the WFC our limiting magnitudes differ slightly from one image to the next. The survey completeness magnitudes are $R = 20.5$, $I = 19.5$, and $Z = 19.2$, while limiting magnitudes are $R = 23.2$, $I = 21.8$, and $Z = 21.0$. In Table 1 we list the limiting and completeness magnitudes for each of the CCDs and regions observed.

For each CCD analyzed we constructed the I vs. $R - I$ and I vs. $I - Z$ color-magnitude (CM) diagrams. These proved useful in distinguishing between cool cluster-member candidates and field stars. Figure 2 shows the resulting I vs. $R - I$ diagram of our survey where we have plotted an arbitrary straight line separating our candidates

¹IRAF is distributed by National Optical Astronomy Observatories, which is operated by the Association of Universities for Research in Astronomy, Inc., under contract with the National Science Foundation.

from field stars. Cluster-member candidates are identified as objects brighter and redder than the Pleiades sequence shifted to the distance of σ Orionis in both CM diagrams. We have selected 46 very low-mass stars and brown dwarf candidates with magnitudes in the interval $I = 15\text{--}20$ mag that were found to be red in both CM diagrams. Table 2 shows the list of our candidates with their magnitudes and coordinates (IAU designations are included). Those objects which do not appear red in both CM diagrams (they are indicated with different symbols in Fig. 2) have not been considered in the following discussions on cluster membership and therefore, they are not listed in Table 2. Nevertheless, it has been shown that the $R - I$ color saturates at a given value ($R - I \sim 2.4$, Bessell 1991) becoming bluer for cooler objects. This value may be dependent on gravity, younger objects saturating at slightly redder colors (see Martín, Rebolo, & Zapatero Osorio 1996; Bouvier et al. 1998). Thus, $R - I$ cannot be used by itself as a good indicator of very faint cluster members, and we rely on the $I - Z$ color for the selection of candidates. The objects in our survey with I magnitudes fainter than 20 mag showing red $I - Z$ colors and $(R - I) \geq 2.1$ are listed in Table 3 (coordinates and IAU designations are given). This table may be not complete since the magnitude range here is clearly beyond the completeness of our survey. Astrometry was carried out using the USNO-SA2.0 catalog (Monet et al. 1996) and the ROE/NRL catalog (Yentis et al. 1992), a precision around 1 arcsec being achieved. The spatial distribution of the candidates within the area surveyed is shown in Fig. 1 and finder charts in the I -band ($3' \times 3'$ in extent) are provided in Fig. 3.

2.2. Spectroscopy

We have obtained low-resolution optical spectroscopy of nine of our photometric candidates (SOri 12, 17, 25, 27, 29, 39, 40, 44, and 45), using the 4.2-m William Herschel Telescope (WHT) at the ORM. The spectra were collected on 1997 December 28–30; the

instrumentation used was the ISIS double-arm spectrograph (the red arm only), the R158R grating and the TEK 1024×1024 pixel² CCD detector which provides a total spectral coverage of 635–920 nm and a nominal dispersion of 2.9 Å per pixel. The spectral resolution (FWHM) of the instrumental setup was 20 Å. Exposure times ranged from 900 to 2500 s depending on the magnitudes of the objects and on the weather conditions. Spectra were reduced by a standard procedure using IRAF, which included debiasing, flat-fielding, optimal extraction, and wavelength calibration using the sky lines appearing in each individual spectrum (Osterbrock et al. 1996). Finally, the spectra were corrected for the instrumental response making use of the standard star G 191-B2B, which has absolute flux data available in the IRAF environment.

All the spectra clearly correspond to late M-type objects, showing typical VO and TiO molecular bands. We have classified them by comparison to Pleiades members of known spectral types (Martín et al. 1996; Zapatero Osorio et al. 1997b) resulting that our objects range from class M6 to M8.5. We have also obtained the pseudo-continuum PC1–4 indices (Martín et al. 1996) and found them to yield slightly earlier spectral types by about half a subclass with respect to the main sequence field dwarfs. This is likely due to an effect of gravity; nevertheless this difference is within the estimated error bar of our measurements. The spectra of eight of the candidates (all except for S Ori 44) are shown in Fig. 4, where the clearest features are indicated.

3. Discussion

3.1. Contamination by other sources

Possible contaminating objects in our survey are red galaxies, M giants, and foreground field M dwarfs. Due to the spatial resolution and completeness magnitudes of our

observations, the contamination due to red galaxies is not a major problem, since these are mostly resolved and routines in IRAF can distinguish them from stellar point-like objects. Another source of contamination is the M giants, but given the galactic latitude of the cluster ($b = -17.34$ deg) their number is negligible ($\leq 5\%$) in comparison with main-sequence dwarfs (Kirkpatrick et al. 1994).

The most relevant source of contamination is field M dwarf stars in the line of sight towards the cluster. To estimate their number we have considered the results from searches covering a large area of the sky. Kirkpatrick et al. (1994) performed a 27.3 deg^2 survey, reaching a completeness magnitude of $R = 19$ mag and finding space densities of 0.0022 pc^{-3} , 0.0042 pc^{-3} , and 0.0024 pc^{-3} for M5–M6, M6–M7, and M7–M9 dwarfs, respectively. With these densities and with the typical absolute magnitudes of late M dwarfs (Kirkpatrick & McCarthy 1994) we have calculated the number of these cool stars that might be populating the CM region which we ascribe to the cluster members. The result is that less than one M5–M6, about one M6–M7, and one M7–M9 field dwarfs should be contaminating our survey. Our selection criterion based on the three filters R , I , and Z appears to be good enough to differentiate clearly between true members and contaminating field stars, but further studies in the near infrared, which is less affected by reddening, or low-resolution spectroscopy will tell us which objects are definitely bona fide cluster members.

3.2. The σ Orionis cluster: size, age, and distance

The existence of a cluster around the multiple star σ Orionis was noted for the first time in the Lund Observatory Catalogue of Open Clusters (Lynga 1981), where it was designated by the name of the star. In later studies (Lynga 1983) about fourteen stars were given as members and the diameter of the cluster in the sky was estimated at 25 arcmin. The work by Wolk (1996) and Walter et al. (1997) covered an area of 900 arcmin^2 containing a

rather dense population of X-ray sources, and found a homogeneous distribution of cluster candidates. In the future, a larger area will need to be surveyed to determine with precision the total region occupied by the cluster, since our current knowledge may be limited to the core.

Age is one of the most important parameters of a cluster, particularly in locating the substellar mass limit. Until recently, the only way to determine the age of σ Orionis was via studies of the massive stars of the OB1b subgroup, resulting in age estimates in the range of 1.7–7 Myr, (Blaauw 1991; WH; BGZ). The discovery by Wolk (1996) of a large low-mass population allowed him to compare H–R diagrams with theoretical isochrones and obtain an age for the cluster of about 2 Myr (Wolk & Walter 1999), in good agreement with estimates for the subgroup, and especially with the age given by the latest work of BGZ (1.7 Myr). This provides additional support for the assumption that the cluster belongs to the young Orion star forming region, and that its central star, σ Orionis, is indeed a member in the cluster of the same name. Figure 5 shows our candidates together with theoretical isochrones from several authors ((*a*) Burrows et al. 1997; (*b*) D’Antona & Mazzitelli 1997; (*c*) Baraffe et al. 1998). The later models provide magnitudes and colors and in order to transform the effective temperatures and luminosities of the models by Burrows et al. (1997) and D’Antona & Mazzitelli (1997) into the observational CM diagrams of Fig. 5, we have used the temperature–color scale and bolometric corrections from Bessell, Castelli & Plez (1998). The cluster candidates seem to imply average ages of ≤ 1 Myr to 3 Myr according to Burrows et al. (1997), and ≤ 1 Myr to 5 Myr according to D’Antona & Mazzitelli 1997). The evolutionary tracks by Baraffe et al. (1998) used in Fig. 5 (*c*) are those named “dusty” models by these authors and they include dust condensation and opacity in the atmospheres of cool objects. While these models predict effective temperatures and luminosities very similar to the other two sets of isochrones, the predicted magnitudes and colors do not fit the observations. Alternative methods for deriving ages could give a more precise age for

σ Orionis. In particular, the Li-luminosity (LL-clock) dating (see e.g. Martín & Montes 1997; Basri 1998), which provides a very good age determination in the case of the Pleiades and α -Persei clusters (Martín et al. 1998b; Stauffer, Schultz & Kirkpatrick 1998; Basri & Martín 1999) can be useful in this case as it will be discussed in section 3.5.

The distance is another important parameter that needs to be known for a cluster. Measurements available in the literature give a distance modulus of 7.8–8 (WH; BGZ) for the subgroup. More recently, *Hipparcos* has provided a distance to the central star of the cluster σ Orionis of 352 pc ($m - M=7.73$), slightly smaller than previous results, but in good agreement with them. We have adopted this value as the cluster distance.

3.3. Spectroscopy of brown dwarf candidates

From the nine objects studied spectroscopically, eight appear to be very probable young cluster members, which implies a high efficiency (89%) for our photometric search strategy. All eight confirmed candidates (listed in Table 4) show spectral types later than M5 (three M6, two M6.5, two M7, and one M8.5). The rejected candidate (SOri 44) is hotter (M6.5) than expected for its given I magnitude and does not show spectral features indicative of the youth of the σ Orionis cluster, such as $H\alpha$ in emission. In Table 4 we give the strengths of the $H\alpha$ and $Na\ I$ lines. In the Pleiades and α Persei clusters the M6.5 spectral type marks the substellar mass limit (Martín et al. 1998b; Basri & Martín 1999), with an uncertainty of about half a subclass. As very low-mass stars and massive brown dwarfs evolve at nearly constant temperature (± 200 K) from several million years to nearly 100 Myr (Baraffe et al. 1998; Burrows et al. 1997; D’Antona & Mazzitelli 1994), we expect that the substellar mass limit is located at a similar spectral type for ages of a few Myr (Luhman et al. 1998a). This should be taken with caution if the relationship between effective temperature and spectral type for low-gravity objects is different from that of dwarfs or 100 Myr old objects. All our

spectroscopically confirmed candidates with spectral types later than M7 are therefore very likely brown dwarfs. In Fig. 6 we can see that the eight objects show indications of strong activity, with higher H α emission than Pleiades objects of the same spectral type. This argues in favor of a younger age, since it is expected that activity decreases with the age. We also see variations in the emission of objects of similar type, a kind of behavior already seen in late M objects of young clusters like the Pleiades, IC 348 or Taurus (Zapatero Osorio et al. 1997b; Luhman et al. 1998b; Briceño et al. 1998). Spectral features associated with Na I and K I can be seen in some spectra, while in others they are too weak and we can only set upper limits. The smaller equivalent width (EW) of Na I in our σ Orionis candidates (except for S Ori 44 which shows an absorption typical of ages older than 100 Myr) with respect to Pleiades and older field objects of the same spectral type may be a result of the lower surface gravity of these very young objects (Martín et al. 1996; Luhman et al. 1997; Briceño et al. 1998).

3.4. The coolest brown dwarf in the σ Orionis cluster

Our candidate of latest spectral type (M8.5), S Ori 45, deserves special attention since it is among the coolest and therefore among the least massive objects in our sample. This very young brown dwarf candidate has an effective temperature in the range between 2100 and 2500 K, as derived from different temperature scales for dwarfs available in the literature (Tinney et al. 1993; Kirkpatrick 1995; Jones et al. 1996; Leggett et al. 1998; Bessell et al. 1998). However, we note that the temperature scale for giants is several hundred degrees warmer and an upward correction in the estimated temperature of about 100–200 K (Luhman et al. 1997) may be required. The luminosity of the object can be obtained from the I magnitude using the bolometric corrections of various authors (Monet et al. 1992; Tinney et al. 1993; Kirkpatrick, Henry & Simons 1995; Bessell & Stringfellow 1993; Bessell

et al. 1998). We derived an average correction factor $BC_1 = -1.1 \pm 0.1$. From a comparison of the colors of our objects with those of objects of the same spectral type in the Pleiades and field stars, we do not find any significant reddening ($A_V \leq 0.5$ mag). So, assuming that the extinction is negligible, and taking as distance modulus of the cluster $m - M = 7.73$, we obtain a luminosity for our object of $\log L/L_\odot = -2.40 \pm 0.15$. If we adopt 10 Myr as an upper limit for its age, according to theoretical calculations of luminosities for young ages (Baraffe et al. 1998; D’Antona & Mazzitelli 1997; Burrows et al. 1997) we infer a mass of 0.020–0.040 M_\odot for S Ori 45, and for the most likely age of the cluster, 2–5 Myr, a mass of only 0.020–0.025 M_\odot . Therefore it is one of the least massive objects found to date outside the Solar System. Follow-up IR and/or spectroscopic observations may reveal even less massive objects among the faintest σ Orionis cluster photometric candidates of Table 3. The uncertainties in the conversion from magnitudes to luminosities and in the theoretical modeling of such low-mass objects at very early ages are considerable, hence this mass estimate is to be treated with caution. Nevertheless, our results leave little doubt concerning the extension of the star formation process very deep in the brown dwarf domain. In Table 4 luminosities and masses are derived using the same procedure given above for the remaining of the eight candidates for which spectra were obtained.

In Fig. 7 we compare our least massive brown dwarf candidate of Table 2, S Ori 45, with other objects of spectral type M8.5 from Ophiuchus, the Pleiades and the field. The stronger $H\alpha$ emission and the much lower strength of K I and Na I lines are noteworthy (Figs. 7(b, c, d)). As mentioned above, this is to be expected for a very young object. Another interesting feature is that the VO and TiO molecular bands are clearly less intense in the field star than in S Ori 45 (see the spectral regions 660–760 nm and 840–880 nm, Fig. 7(c)). This is possibly a consequence of the higher gravity of the older systems, which favors the condensation of dust grains in cold atmospheres (Tsuji, Ohnaka, & Aoki 1996). In Fig. 7(a) we show a comparison with the spectrum of the M8.5 object found by Luhman

et al. (1997) in Ophiuchus. The similarity of the two spectra is remarkable. These two objects, although discovered in star forming regions far away from each other, appear to be extremely similar, suggesting that low-mass brown dwarfs could be quite common. Old counterparts of these substellar objects may be populating the galactic disk. At the age of a few Gyr their atmospheric temperatures will be similar to or likely lower than that of Gl 229B (~ 1000 K), so it is expected that they present spectroscopic characteristics intermediate between those of Gl 229B and Jupiter. Important questions that remain unanswered are how many objects of this kind there are, and whether even less massive ones can form. These questions are obviously related to our knowledge of the mass function at such low masses, but beyond the scope of this article. Although we believe that the area covered and the number of objects are significant, at this juncture this issue presents several difficulties mainly due to the uncertainty in the cluster age; small changes in the adopted age imply a significantly different mass-luminosity relationship and consequently, large variations in the slope of the mass function. To this difficulty we must add the uncertainty in the membership of our candidates, especially the faintest ones, which might be more contaminated by reddened field stars. Nevertheless, if we adopt the age (about 3 Myr) of the model which provides the best fit to the optical photometric sequence of σ Orionis we derive that the number of brown dwarfs per unit of mass grows through the substellar domain till around $0.040 M_{\odot}$, which is in agreement with what is seen in the Pleiades (Martín et al. 1998c; Bouvier et al. 1998).

3.5. Lithium and deuterium depletion: prospects of identification of substellar objects and age determination

Young stellar clusters such as σ Orionis are excellent laboratories for studying the depletion of light elements such as deuterium, lithium, berillium, and boron, since these

elements are burned in the early stages of pre-main sequence stellar evolution and their atmospheric abundances drastically change in this phase. As mentioned before, a detailed knowledge of lithium burning at the bottom of the main sequence has provided an alternative method of age determination for the young clusters α Persei and the Pleiades. This method appears to be more reliable than traditional ones, based on evolutionary models of the more massive stars in the clusters which are limited by our poor knowledge of the interiors of these stars. Lithium dating relies on the fact that in fully convective low-mass stars lithium burning takes place over a very short time interval (a few Myr) once the temperature in the core is high enough to produce the destructive reactions $(\text{Li,p})\alpha$. The lower the mass of the star the greater is the age at which it starts lithium burning; in any case this age is always smaller than a few tens of Myr. Brown dwarfs less massive than $0.060\text{--}0.065 M_{\odot}$ do not ever burn lithium because their cores do not reach the minimum burning temperature. The presence of lithium in the atmosphere of low luminosity, fully convective objects is a clear indication that the maximum internal temperature is below the lithium burning value, and that the object is sub-stellar. However this simple criterion can be applied only if the object is older than 150 Myr. Those objects with masses above $0.065 M_{\odot}$ do destroy lithium while they are young (≤ 150 Myr) and this fact can be used for dating clusters.

A detailed inspection of evolutionary models confirms that the transition between lithium depletion/preservation in the atmospheres of low-mass objects takes place at higher masses and luminosities as we consider younger ages. Given the youth of σ Orionis, this transition should occur in early/mid M-type stars. If the age were indeed 10 Myr we would expect stars in the mass range $0.9\text{--}0.4 M_{\odot}$ ($-1.0 \leq \log L/L_{\odot} \leq -0.5$) to have burned most of their original lithium content, whereas if the cluster is as young as 2–5 Myr, neither stars nor massive brown dwarfs would have had sufficient time to reach the interior temperatures needed to start lithium burning (D’Antona & Mazzitelli 1997; Soderblom et al. 1998). It

is consequently very important to search for lithium in the early/mid M-type stars of the cluster.

The Deuterium Test

Deuterium has a similar behavior to that of Li as it is a light element that is destroyed in stellar interiors when the temperature reaches 0.8×10^6 K (Ventura & Zeppieri 1998), i.e., much below the minimum temperature for lithium burning. Therefore, deuterium burning takes place at much earlier ages and extends to less massive substellar objects (0.015 – $0.018 M_{\odot}$, Burrows et al. 1993; D’Antona & Mazzitelli 1997; Burrows et al. 1997). Brown dwarfs with masses larger than $0.02 M_{\odot}$ efficiently destroy deuterium in the age range 1–10 Myr and this destruction takes place on a very short time scale. Figure 8 represents the evolution of the deuterium abundance as a function of age for several masses. Only objects below $0.02 M_{\odot}$ can preserve their original abundance on time scales of 10 Myr, since it will take longer for them to burn any deuterium. During the deuterium-burning phase the luminosity and effective temperatures stay almost constant (Burrows et al. 1993; D’Antona & Mazzitelli 1994). All the physical arguments discussed above for lithium can be applied to deuterium. There is a transition between objects which have burned deuterium and those which have preserved it which in principle can provide an age determination method. In Fig. 8, we can note, as an example, how an object of 0.07 – $0.08 M_{\odot}$ with an age of 3 Myr has destroyed a significant amount of its initial deuterium abundance, whereas a $0.03 M_{\odot}$ object does not burn deuterium (by a factor larger than 10) until an age of 7 Myr. If σ Orionis were as young as 2–3 Myr the transition between deuterium burning and preservation would take place at $\log L/L_{\odot} = -1.6$ which approximately coincides with the substellar mass limit (0.070 – $0.075 M_{\odot}$), while at an age of 10 Myr the deuterium preservation would take place at $\log L/L_{\odot} \sim -3$ (D’Antona & Mazzitelli 1997). We have considered theoretical models with the interstellar abundance of deuterium (see e.g. Linsky 1998) for this discussion. If the initial abundance of this isotope is changed by 50%, the

time scale for the deuterium depletion is subsequently affected by a factor ~ 1.5 . For a given age the lower the abundance of deuterium is, the lower the luminosity and the mass at the deuterium depletion/preservation boundary.

It is interesting to note that at the approximate age of 4 Myr, all low-mass stars will have destroyed their deuterium by several orders of magnitude; therefore, the simple detection of this isotope in an older object would manifest its substellar nature. The detection of deuterium, then, complements that of lithium as a test of substellarity for young objects and provides a way of confirming the substellar nature of objects which, due to their young ages, cannot be confirmed as such by the lithium test. We shall also note an alternative way to make use of the potential of deuterium observations: any object older than 1 Myr, with a luminosity below $\log L/L_{\odot} = -1.5$ and where deuterium is preserved, must be substellar.

The detection of deuterium is difficult and presents an important challenge from the observational point of view. Deuterium has been detected in the planets and comets of the Solar System among other astrophysical sites. The observations were made using dipole lines of monodeuterated hydrogen in the visible (Macy & Smith 1978) and rotational bands of monodeuterated methane at $1.6 \mu\text{m}$ (De Bergh et al. 1986, 1988, 1990). Implications on primordial deuterium could be deduced if detection were achieved in young brown dwarfs, or in those less massive than $0.015 M_{\odot}$. The very low-mass σ Orionis cluster members are in the phase of burning this light element. Figure 9 shows our candidates in an H–R diagram, which includes the frontier between the depletion (by a factor 10) and preservation of deuterium for different ages. To convert I magnitudes and colors to luminosities and temperatures, we have taken account of the same references given in §3.4. As we can see, if the cluster were indeed as young as it has been claimed (around 3 Myr), all objects with luminosities below $\log L/L_{\odot} = -1.7$ and temperatures cooler than ~ 2700 K (about M6–M7

spectral types) could preserve their deuterium, while if the cluster were as old as 10 Myr, this could happen only to those with the latest types. Objects like S Ori 45 are then the most promising candidates for detecting deuterium. Observations of deuterium in a substantial number of σ Orionis members could also be used to constrain any age spread within the cluster.

4. Conclusions

We have performed a deep R , I , and Z survey in the very young cluster σ Orionis covering an area of 870 arcmin^2 and have found objects with masses as small as $0.020\text{--}0.025 M_{\odot}$, well below the substellar mass limit. Our selected 49 candidates define a photometric sequence ranging in age from ≤ 1 Myr to 5 Myr, which is in agreement with previous results for the OB1b subgroup, where the multiple star σ Orionis is associated.

We have confirmed spectroscopically the cool nature of eight of these objects (spectral types M6–M8.5), which show spectral features indicative of a stronger activity and lower gravity than previously known members of similar types in older clusters. Our latest candidate, S Ori 45 (M8.5), is one of the least-massive objects known to date, with a best estimate of its mass at $0.020\text{--}0.025 M_{\odot}$ for the age of 2–5 Myr. An upper limit of $0.040 M_{\odot}$ is estimated if the age of the cluster were as old as 10 Myr. The detection of the old counterparts of these brown dwarfs in the solar neighborhood will represent a challenge for future searches as they will cool down to very low atmospheric temperatures ($T_{\text{eff}} \lesssim 1000 \text{ K}$). At the age of the Sun a brown dwarf of $0.020 M_{\odot}$ may have absolute magnitudes of around $M_J \sim 20\text{--}21$, and $M_K \sim 22\text{--}23 \text{ mag}$ (Burrows et al. 1997). Given the limiting magnitudes of the current large scale infrared surveys like DENIS (Delfosse et al. 1999) and 2MASS (Beichman et al. 1998), the detection of such low-mass brown dwarfs would be possible if they were located at distances closer than about 3 pc.

The study of light elements like lithium and deuterium in brown dwarfs of young clusters may provide a precise tool of determining ages. In particular, the least-massive brown dwarfs that we have found in σ Orionis should have preserved their deuterium and it is worthwhile investigating possible ways of achieving its detection.

Acknowledgments: We thank A. Oscoz for acquiring data at the IAC-80 Telescope necessary for the calibration photometry of the WFC observations. We thank K. Luhman for kindly have provided the M8.5 spectrum in ρ Ophiuchi, and I. Baraffe and the Lyon group and F. D’Antona for sending us electronic versions of their recent models. This work is based on observations obtained at the INT and WHT operated by the Isaac Newton Group of Telescopes funded by PPARC at the Spanish Observatorio del Roque de los Muchachos of the Instituto de Astrofísica de Canarias and the IAC80 Telescope at the Observatorio del Teide (Tenerife, Spain). Partial financial support was provided by the Spanish DGES project no. PB95-1132-C02-01.

REFERENCES

- Alcalá, J. M., Chavarría-K., C., & Terranegra, L. 1998, *A&A*, 330, 1017
- Alcalá, J. M., et al. 1996, *A&ASS*, 119, 7
- Baraffe, I., Chabrier, G., Allard, F., & Hauschildt, P. H. 1998, *A&A*, 337, 403
- Basri, G. 1998, in *ASP Conf. Ser. Vol. 134, Brown Dwarfs and Extrasolar Planets*, eds R. Rebolo, E. L. Martín, & M. R. Zapatero Osorio (San Francisco: ASP), p. 394
- Basri, G., and Martín, E. L. 1999, *ApJ*, in press
- Beichman, C. A., Chester, T. J., Skrutskie, M., Low, F. J., Gillett, F. 1998, *PASP*, 110, 480
- Bessell, M. S., Castelli, F., & Plez, B. 1998, *A&A*, 333, 231
- Bessell, M. S., & Stringfellow, G. S. 1993, *ARA&A*, 31, 433
- Bessell, M. S. 1991, *AJ*, 101, 662
- Blaauw, A. 1964, *ARA&A*, 2, 213
- Blaauw, A. 1991, in *NATO/ASI Series C, Vol. 342, Physics of Star Formation and Early Stellar Evolution*, eds C. J. Lada & N. D. Kylafis, p. 125
- Bouvier, J., Stauffer, J. R., Martín, E. L., Barrado y Navascúes, D., Wallace, B., & Béjar, V. J. S. 1998, *A&A*, 336, 490
- Briceño, C., Hartmann, L., Stauffer, J., & Martin, E. L. 1998, *AJ*, 115, 2074
- Brown, A. G. A., de Geus, E. J., & de Zeeuw, P. T. 1994, *A&A*, 289, 101 (BGZ)
- Burrows, A., Hubbard, W. B., Saumon, D., & Lunine, J. I. 1993, *ApJ*, 406, 158
- Burrows, A., et al. 1997, *ApJ*, 491, 856

Cossburn, M. R., Hodgkin, S. T., Jameson, R. F., & Pinfield, D. J. 1997, MNRAS, 288, L23

D’Antona, F., & Mazzitelli, I. 1994, ApJS, 90, 467

D’Antona, F., & Mazzitelli, I. 1997, ‘Evolution of low mass stars’ in “Cool stars in Clusters and Associations”, eds. G. Micela and R. Pallavicini, Mem. S.A.It., 68, 807

De Berg, C., Chauville, J., Lutz, B. L., Owen, T., & Brault, J. 1986, ApJ, 311, 501

De Berg, C., Lutz, B. L., Owen, T., & Chauville, J. 1988, ApJ, 329, 951

De Berg, C., Lutz, B. L., Owen, T., & Maillard, J. 1990, ApJ, 355, 661

Delfosse, X., Tinney, C. G., Forveille, T., Epchtein, N., Borsenberger, J., Fouqué, P., Kimeswenger, S., Tiphène, D. 1999, A&AS, in press

Jones, H. R. A., Longmore, A. J., Allard, F., & Hauschildt, P. H. 1996, MNRAS, 280, 77

Kirkpatrick, J. D. 1995, , in “The Bottom of the Main Sequence, and Beyond”, ESO Workshop, ed. C.G. Tinney (Springer-Verlag), p.140.

Kirkpatrick, J. D., Henry, T. J., & Simons, D. A. 1995, AJ, 109, 797

Kirkpatrick, J. D., & McCarthy, D. W. 1994, AJ, 107, 333

Kirkpatrick, J. D., McGraw, J. T., Hess, T. R., Liebert, J., & McCarthy, D. W. 1994, ApJS, 94, 749

Kogure, T., Yoshida, S., Wiramihardja, S. D., Nakano, M., Iwata, T., & Ogura, K. 1989, PASJ, 41, 1195

Landolt, A. U. 1992, AJ, 104, 340

Lee, T. A. 1968, ApJ, 152, 913

- Leggett, S. K., Allard, & Hauschildt, P. H. 1998, *ApJ*, 509, 836
- Linsky, J. L. 1998, *Space Science Reviews*, 84, 285
- Luhman, K. L., Briceño, C., Rieke, G. H., & Hartmann, L. 1998, *ApJ*, 493, 909
- Luhman, K. L., Liebert, J., & Rieke, G. H. 1997, *ApJ*, 489, L165
- Luhman, K. L., Rieke, G. H., Lada, C. J., & Lada, E. A. 1998b, *ApJ*, 508, 347
- Lynga, G. 1981, *Catalog of Open Cluster Data*
- Lynga, G., 1983, in *Ceskoslovenska Akademie Ved Fifth Conf. on Star Clusters and Assoc. and their Relation to the Evolution of the Galaxy*, p. 80
- Macy, W. J., & Smith, W. H., 1978, *ApJ*, 222, L73
- Martín, E. L., Basri, G., Gallegos, J. E., Rebolo, R., Zapatero Osorio, M. R., & Béjar, V. J. S. 1998b, *ApJ*, 499, L61
- Martín, E. L., Basri, G., Zapatero Osorio, M. R., Rebolo, R., and García López, R. J. 1998a, *ApJ*, 507, L41
- Martín, E. L., & Montes, D. 1997, *A&A*, 318, 805
- Martín, E. L., Rebolo, R., & Zapatero Osorio, M. R. 1996, *ApJ*, 469, 706
- Martín, E. L., Zapatero Osorio, M. R., & Rebolo, R. 1998c, in *ASP Conf. Ser. Vol. 134, Brown Dwarfs and Extrasolar Planets*, eds R. Rebolo, E. L. Martín, & M. R. Zapatero Osorio (San Francisco: ASP), 394
- Monet, D. G., Dahn, C. C., Vrba, F. J., Harris, H. C., Pier, J. R., Luginbuhl, C. B., & Ables, H. D. 1992, *ApJ*, 103, 638

- Monet, D., Bird, A., Canzian, B., et al. 1996, USNO-SA2.0, (U.S. Naval Observatory, Washington DC).
- Osterbrock, D. E., et al. 1996, PASP, 108, 277
- Rebolo, R., Zapatero Osorio, M. R., & Martín, E. L. 1995, Nature, 377, 129
- Soderblom, D. R., et al. 1998, ApJ, 498, 385
- Stauffer, J., Schultz, G., and Kirkpatrick, J. D. 1998, ApJ, 499, L199
- Sterzik, M. F., Alcalá, J. M., Neuhauser, R., & Schmitt, J. H. M. M. 1995, A&A, 297, 418
- Tinney, C. G., Mould, J. R., & Reid, N. 1993, AJ, 105, 1045
- Tsuji, T., Ohnaka, K., & Aoki, W. 1996, ApJ, 305, L1
- Ventura, P., and Zeppieri, A. 1998, A&A, 340, 77
- Walter, F. M., Vrba, F. J., Mathieu, R. D., Brown, A., & Myers. 1994, AJ, 107, 692
- Walter, F. M., Wolk, S. J., Freyberg, M., Scmitt, J. H. M. M. 1997, “Cool Stars in Clusters and Associations: Magnetic Activity and Age Indicators”, *Memorie della Società Astronomica Italiana*, Vol. 68, p. 1081
- Warren, W. H., & Hesser, J. E. 1978, ApJS, 36, 497 (WH)
- Wiramihardja, S. D., Kogure, T., Yoshida, S., Nakano, M., Ogura, K., & Iwata, T. 1991, PASJ, 43, 27
- Wiramihardja, S. D., Kogure, T., Yoshida, S., Ogura, K., & Nakano, M. 1989, PASJ, 41, 155
- Wiramihardja, S. D., Kogure, T., Yoshida, S., Ogura, K., & Nakano, M. 1993, PASJ, 45, 643

Wolk, S. J. 1996, PhD thesis, University of New York at Stony Brook

Wolk, S. J., & Walter, F. M., 1999, in “Very Low-Mass Stars and Brown Dwarfs in Stellar Clusters and Associations”, eds R. Rebolo & M. R. Zapatero Osorio, in preparation

Yentis, D. J., Cruddace, R. G., Gursky, H., Stuart, B. V., Wallin, J. F., MacGillivray, H. T., and Collins, C. A. 1992 in “Digitised Optical Sky Surveys”, H. T. MacGillivray and E.B. Thomson, Kluwer, Dordrecht, 67

Zapatero Osorio, M. R., Rebolo, R., & Martín, E. L. 1997a, *A&A*, 317, 164

Zapatero Osorio, M. R., Rebolo, R., Martín, E. L., Basri, G., Magazzù, A., Hogdkin, S. T., Jameson, R. F., & Cossburn, M. R. 1997b, *ApJ*, 491, L81

Zapatero Osorio, M. R., Rebolo, R., Martín, E. L., Hodgkin, S. T., Cossburn, M. R., Magazzù, A., Steele, I. A., and Jameson, R. F. 1998, *A&AS*, in press

Fig. 1.— Location of our fields (open squares) covering an area of 870 arcmin^2 around the multiple star σ Orionis (indicated with a cross). Filled symbols represent our candidates (Tables 2 and 3) and open circles denote those stars in the field brighter than 13 mag. The relative brightness is denoted by circle diameters. North is up and East is left.

Fig. 2.— Color-magnitude diagram for very low-mass stars and brown dwarfs in the σ Orionis cluster resulting from our survey. Filled circles denote our 46 candidates listed in Table 2. Those objects that were not found red in all colors are indicated with open symbols; the ones with $R - I$ measured in Table 3 are shown with open squares. The straight, vertical line separates cluster member candidates from field objects (see text). Completeness and limiting magnitudes are indicated with a dashed line and a full line, respectively.

Fig. 3.— Finder charts in the I -band ($3' \times 3'$ in extent). North is up and East is left.

Fig. 4.— Low-resolution (20 \AA) optical spectra of eight of our candidates normalized at 813 nm. A constant step of 0.8 units has been added to each spectrum for clarity.

Fig. 5.— Color-magnitude diagram for our σ Orionis candidates compared with the recent evolutionary tracks of (a) Burrows et al. (1997), (b) D’Antona & Mazzitelli (1997), and (c) Baraffe (1998). Ages and masses in solar units are indicated. Filled circles denote the candidates listed in Tables 2 and 3, and those objects with spectra presented in this paper are indicated with open triangles. Bright stars ($I \leq 15 \text{ mag}$, open circles) are taken from Wolk (1996), those ones which are confirmed spectroscopically.

Fig. 6.— The NaI and $H\alpha$ equivalent widths measured in our σ Orionis candidates (filled circles), in some Pleiades members (open squares) and in some field stars (open triangles) plotted against spectral type. Error bars of our measurements are indicated in the upper right corner.

Fig. 7.— Our candidate S Ori 45 (M8.5 spectral type, full line) compared to its spectral type counterpart (dashed line) in (a) Ophiuchus (Luhman et al. 1997), (b) the Pleiades, and (c) the field. The Pleiades spectrum has been obtained averaging those of the brown dwarfs Teide 1 (M8, Martín et al. 1996) and Roque 4 (M9, Zapatero Osorio et al. 1997b). In panel (d) an enlargement of the Na I doublet is presented where S Ori 45 is denoted with a full line, and the Pleiades and field M8.5-type spectra are plotted with dashed and dotted lines, respectively.

Fig. 8.— The deuterium burning as a function of age (models of D’Antona & Mazzitelli 1998, those with the interstellar abundance of deuterium). Masses are indicated in solar units.

Fig. 9.— The HR diagram for our σ Orionis candidates (open circles). D’Antona & Mazzitelli’s (1998) theoretical isochrones of 1, 3 and 10 Myr are superimposed. The borderline for the deuterium depleted by one order of magnitude (90% preservation, and interstellar initial deuterium abundance) is indicated with the dashed line. The cross symbol stands for the location of this borderline at the age of 3 Myr ($\sim 0.060 M_{\odot}$).

Table 1: Completeness and limiting magnitudes

Fields	R.A.	Decl.	Completeness			Limiting		
			<i>R</i>	<i>I</i>	<i>Z</i>	<i>R</i>	<i>I</i>	<i>Z</i>
1	5 39 21	–2 27 00	20.5	19.5	19.0	21.8	20.8	20.2
2	5 38 25	–2 27 00	20.5	19.5	19.0	21.8	20.8	20.2
3	5 39 21	–2 41 00	20.2	19.2	19.2	21.2	20.2	20.2
4	5 37 03	–2 29 00	22.5	20.7	20.2	23.8	22.2	21.5
5	5 38 00	–2 43 00	21.0	20.2	19.7	22.2	21.0	20.5
6	5 38 00	–2 29 00	22.5	20.7	20.2	23.8	22.2	21.5

Note. — Units of right ascension (J2000) are hours, minutes, and seconds, and units of declination (J2000) are degrees, arcminutes, and arcseconds.

Table 2. *RIZ* member candidates in the σ Orionis cluster

ID	IAU	I	$R-I$	R.A. (J2000)	Decl. (J2000)
SOri 1	SOri J053911.7–022741	15.08±0.04	1.70±0.07	5 39 11.7	–02 27 41
SOri 2	SOri J053926.2–022838	15.12±0.04	1.80±0.07	5 39 26.2	–02 28 38
SOri 3	SOri J053920.8–023035	15.16±0.04	2.15±0.07	5 39 20.8	–02 30 35
SOri 4	SOri J053939.2–023227	15.23±0.04	2.16±0.07	5 39 39.2	–02 32 27
SOri 5	SOri J053920.1–023826	15.40±0.05	1.86±0.07	5 39 20.1	–02 38 26
SOri 6	SOri J053847.5–023038	15.53±0.04	2.00±0.07	5 38 47.5	–02 30 38
SOri 7	SOri J053908.1–023230	15.63±0.04	2.07±0.07	5 39 08.1	–02 32 30
SOri 8	SOri J053907.9–022848	15.74±0.04	1.87±0.07	5 39 07.9	–02 28 48
SOri 9	SOri J053817.1–022228	15.81±0.04	2.06±0.07	5 38 17.1	–02 22 28
SOri 10	SOri J053944.4–022445	16.08±0.04	1.97±0.07	5 39 44.4	–02 24 45
SOri 11	SOri J053944.2–023305	16.15±0.04	2.21±0.07	5 39 44.2	–02 33 05
SOri 12	SOri J053757.4–023845	16.28±0.07	1.94±0.09	5 37 57.4	–02 38 45
SOri 13	SOri J053813.1–022410	16.35±0.04	2.05±0.07	5 38 13.1	–02 24 10
SOri 14	SOri J053937.5–024431	16.35±0.05	2.23±0.08	5 39 37.5	–02 44 31
SOri 15	SOri J053848.0–022854	16.55±0.04	2.05±0.08	5 38 48.0	–02 28 54
SOri 16	SOri J053915.0–024048	16.60±0.05	2.15±0.08	5 39 15.0	–02 40 48
SOri 17	SOri J053904.4–023835	16.80±0.05	2.02±0.08	5 39 04.4	–02 38 35
SOri 18	SOri J053825.6–023122	16.81±0.04	2.11±0.08	5 38 25.6	–02 31 22
SOri 19	SOri J053721.0–022543	16.81±0.04	2.12±0.07	5 37 21.0	–02 25 43
SOri 20	SOri J053907.4–022908	16.88±0.04	2.12±0.08	5 39 07.4	–02 29 08
SOri 21	SOri J053934.2–023847	16.90±0.05	2.17±0.09	5 39 34.2	–02 38 47
SOri 22	SOri J053835.2–022524	16.98±0.04	2.24±0.08	5 38 35.2	–02 25 24

Table 2—Continued

ID	IAU	I	$R-I$	R.A. (J2000)	Decl. (J2000)
SOri 23	SOri J053751.0–022610	17.00±0.04	2.23±0.07	5 37 51.0	–02 26 10
SOri 24	SOri J053755.6–022434	17.00±0.04	2.15±0.07	5 37 55.6	–02 24 34
SOri 25	SOri J053908.8–023958	17.04±0.05	2.29±0.11	5 39 08.8	–02 39 58
SOri 26	SOri J053916.6–023827	17.05±0.05	2.04±0.09	5 39 16.6	–02 38 27
SOri 27	SOri J053817.3–024024	17.07±0.05	2.13±0.07	5 38 17.3	–02 40 24
SOri 28	SOri J053923.1–024656	17.11±0.05	2.15±0.09	5 39 23.1	–02 46 56
SOri 29	SOri J053829.5–022517	17.18±0.04	2.03±0.08	5 38 29.5	–02 25 17
SOri 30	SOri J053913.0–023751	17.25±0.05	1.90±0.09	5 39 13.0	–02 37 51
SOri 31	SOri J053820.8–024613	17.31±0.05	2.15±0.07	5 38 20.8	–02 46 13
SOri 32	SOri J053943.5–024731	17.36±0.05	2.04±0.09	5 39 43.5	–02 47 31
SOri 33	SOri J053657.9–023522	17.38±0.04	2.28±0.07	5 36 57.9	–02 35 22
SOri 34	SOri J053707.1–023246	17.46±0.04	2.01±0.07	5 37 07.1	–02 32 46
SOri 35	SOri J053755.5–023308	17.50±0.04	2.36±0.07	5 37 55.5	–02 33 08
SOri 36	SOri J053926.8–023656	17.67±0.06	2.18±0.14	5 39 26.8	–02 36 56
SOri 37	SOri J053707.5–022717	17.70±0.04	2.31±0.07	5 37 07.5	–02 27 17
SOri 38	SOri J053915.1–022152	17.70±0.05	2.13±0.10	5 39 15.1	–02 21 52
SOri 39	SOri J053832.4–022958	17.82±0.05	2.34±0.11	5 38 32.4	–02 29 58
SOri 40	SOri J053736.4–024157	17.93±0.05	2.34±0.07	5 37 36.4	–02 41 57
SOri 41	SOri J053938.4–023116	18.44±0.06	2.43±0.18	5 39 38.4	–02 31 16
SOri 42	SOri J053923.3–024057	19.01±0.09	2.47±0.41	5 39 23.3	–02 40 57
SOri 43	SOri J053813.8–023504	19.05±0.04	2.38±0.08	5 38 13.8	–02 35 04
SOri 44	SOri J053807.0–024321	19.39±0.06	2.31±0.15	5 38 07.0	–02 43 21

Table 2—Continued

ID	IAU	I	$R-I$	R.A. (J2000)	Decl. (J2000)
SOri 45	SOri J053825.5-024836	19.59 ± 0.06	2.88 ± 0.18	5 38 25.5	-02 48 36
SOri 46	SOri J053651.7-023254	19.82 ± 0.04	2.61 ± 0.11	5 36 51.7	-02 32 54

Note. — Units of right ascension (J2000) are hours, minutes, and seconds, and units of declination (J2000) are degrees, arcminutes, and arcseconds. Coordinates are accurate to $\pm 1''$.

Table 3. IZ ($I \geq 20$) member candidates in the σ Orionis cluster

ID	IAU	I	$I - Z$	$R - I$	R.A. (J2000)	Decl. (J2000)
SOri 47	SOri J053814.5–024016	20.53 ± 0.05	1.00 ± 0.06	2.4 ± 0.3	5 38 14.5	–02 40 16
SOri 48	SOri J053739.0–023950	20.70 ± 0.05	0.93 ± 0.08	2.2 ± 0.2	5 37 39.0	–02 39 50
SOri 49	SOri J053822.9–023755	20.83 ± 0.07	1.01 ± 0.08	≥ 1.5	5 38 22.9	–02 37 55

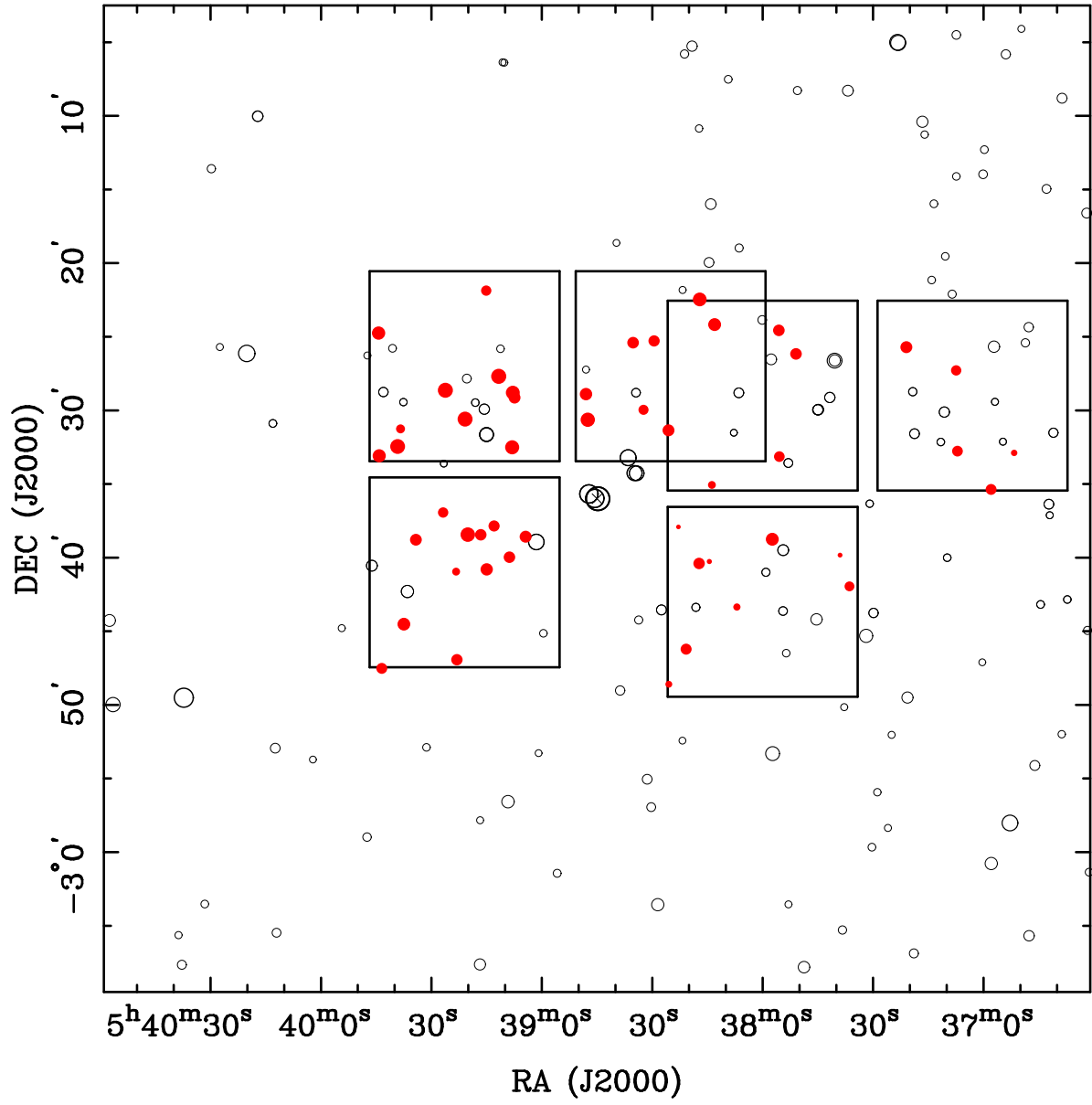
Note. — Units of right ascension (J2000) are hours, minutes, and seconds, and units of declination (J2000) are degrees, arcminutes, and arcseconds. Coordinates are accurate to $\pm 1''$. The Z magnitudes have been calibrated as explained in Zapatero Osorio et al. (1998). Finder charts are available upon request to the authors.

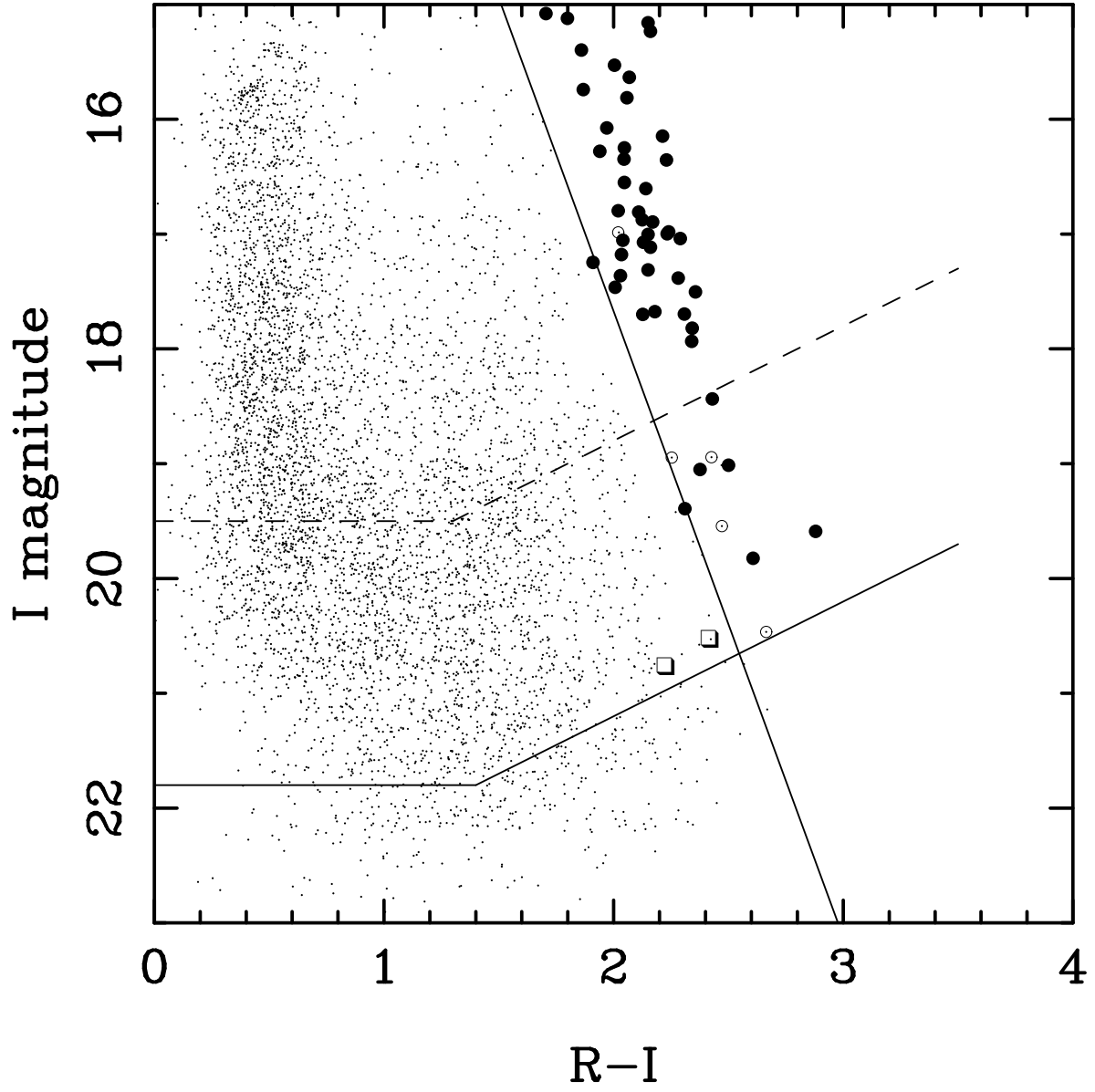
Table 4. Spectroscopic data and fundamental parameters

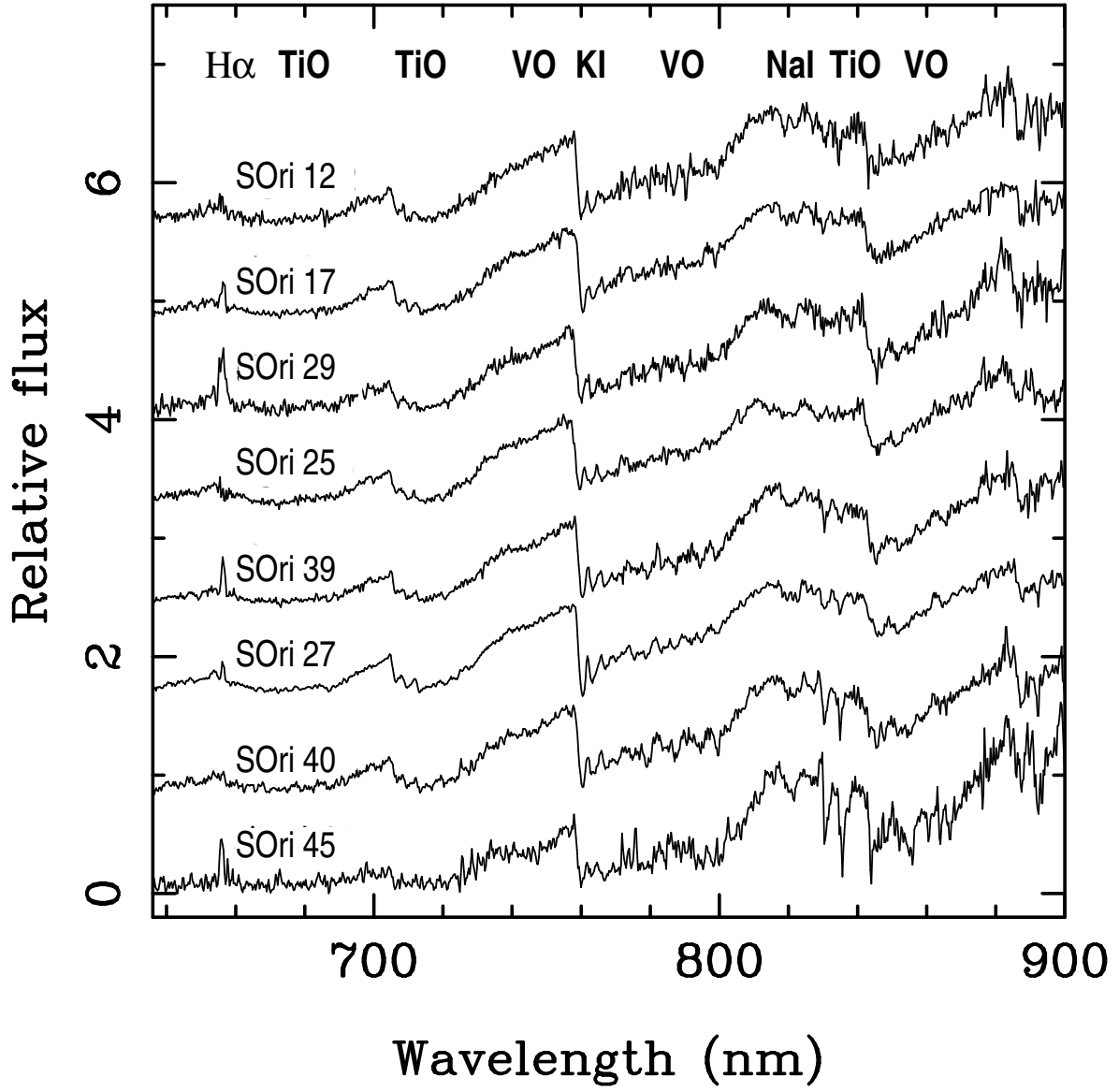
ID	I	SpT	Na I (\AA)	H α (\AA)	$\log L/L_{\odot}$ (± 0.15)	M/M_{\odot} (1–10 Myr)
S Ori 12	16.28	M6.0	2.5	6.5	–1.45	0.070–0.200
S Ori 17	16.80	M6.0	≤ 1.0	5.5	–1.65	0.055–0.150
S Ori 29	17.18	M6.0	2.2	28.0	–1.81	0.045–0.110
S Ori 25	17.04	M6.5	≤ 1.0	45.0	–1.72	0.050–0.130
S Ori 39	17.82	M6.5	≤ 1.0	5.1	–2.02	0.040–0.080
S Ori 27	17.07	M7.0	≤ 1.0	6.1	–1.66	0.055–0.150
S Ori 40	17.93	M7.0	≤ 1.0	30.0	–2.00	0.040–0.080
S Ori 44*	19.39	M6.5	5.0	≤ 5	–	–
S Ori 45	19.59	M8.5	≤ 1.0	60.0	–2.40	0.020–0.040

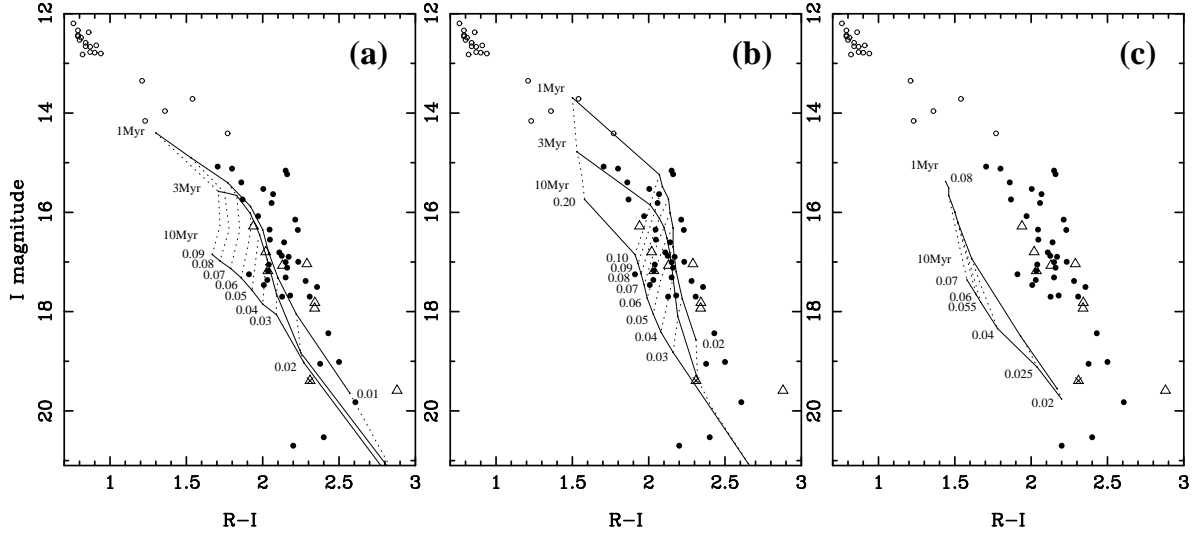
Note. — Uncertainties in spectral types are half a subclass; in EWs they are $\pm 1 \text{\AA}$.

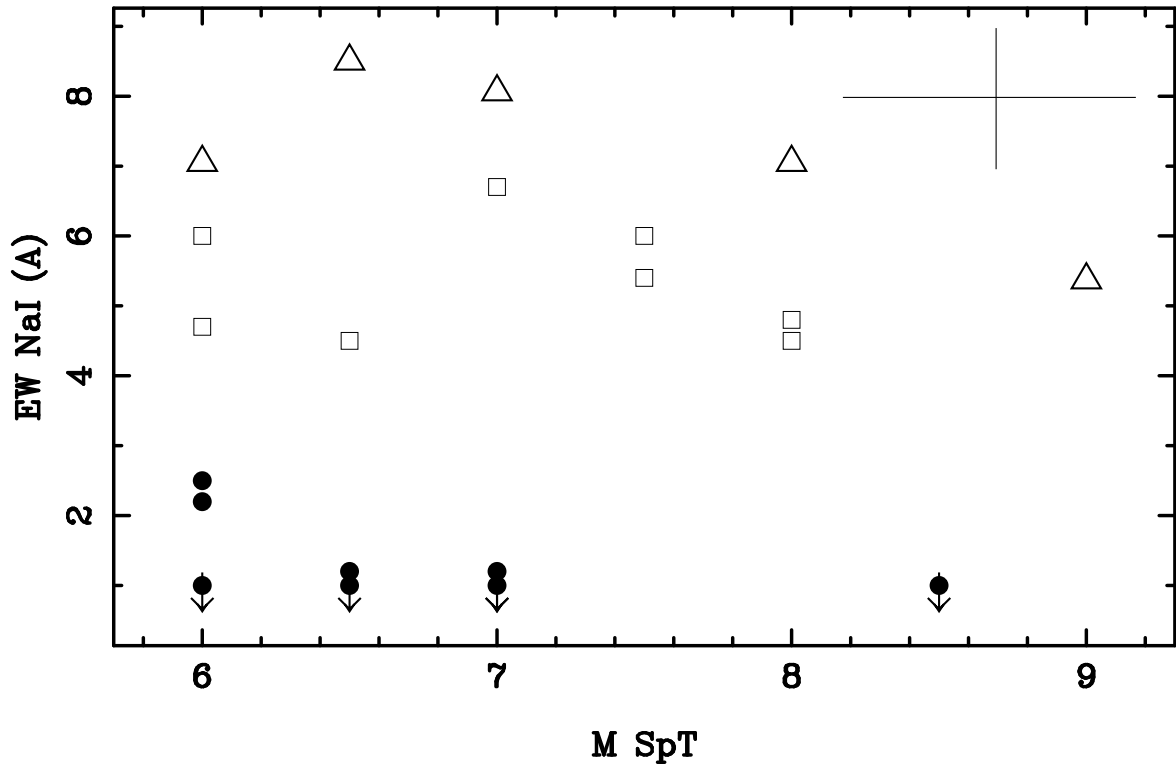
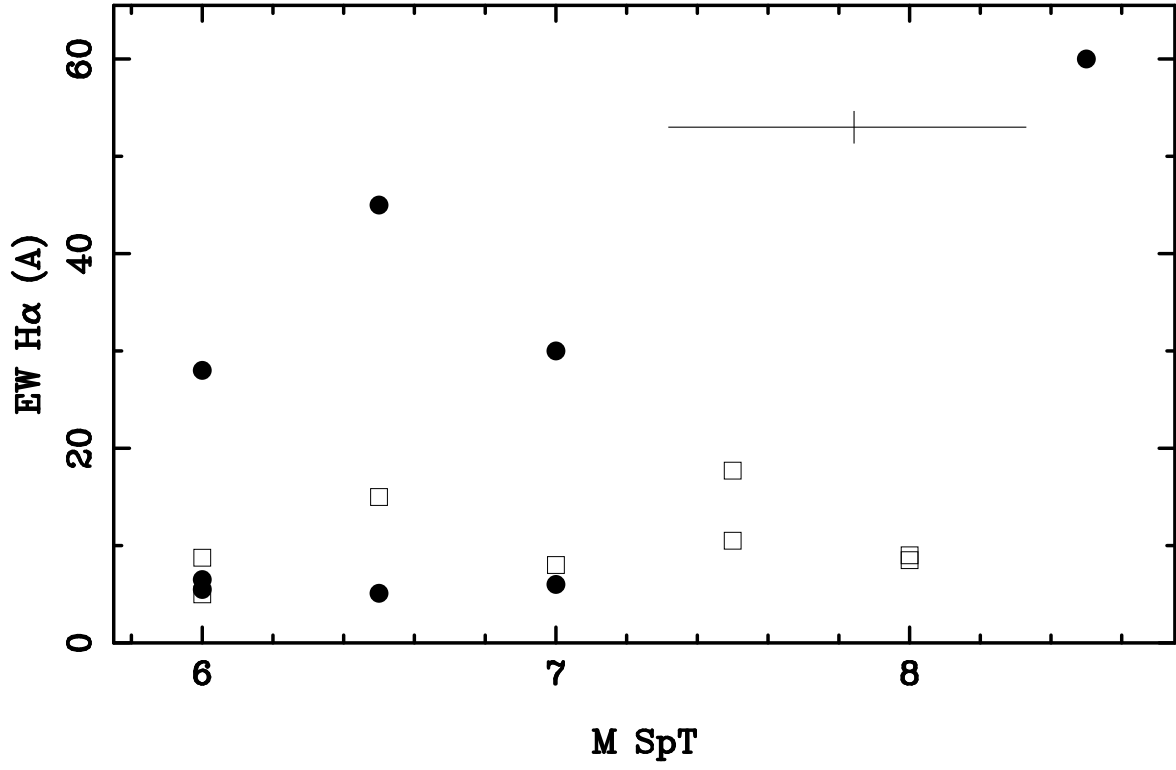
* This object does not show spectroscopic features distinctive of the youth of the σ Orionis cluster, and therefore it has not been considered for the determination of luminosity and mass.

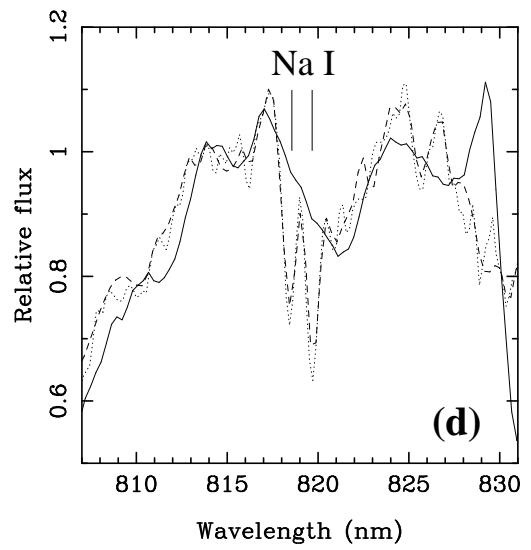
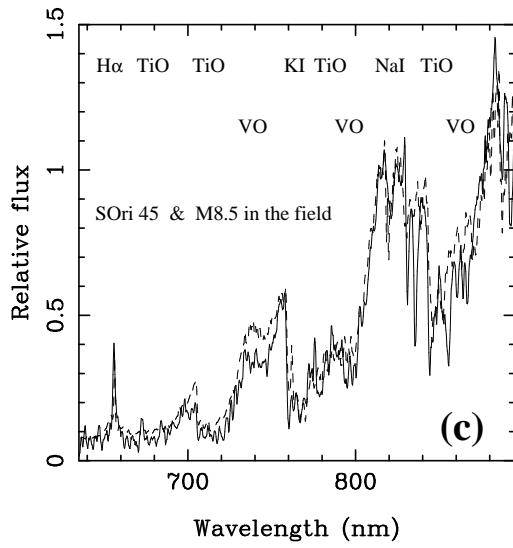
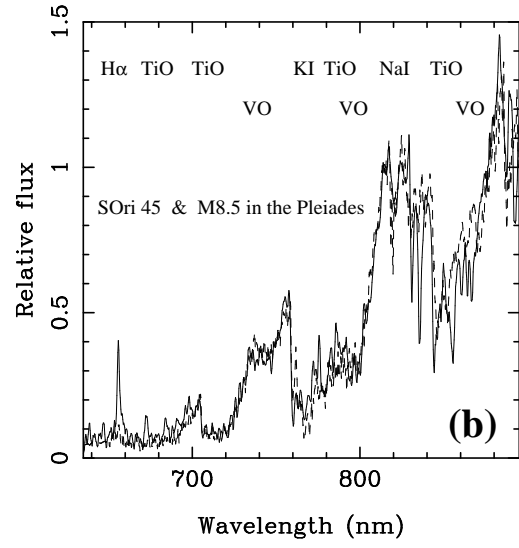
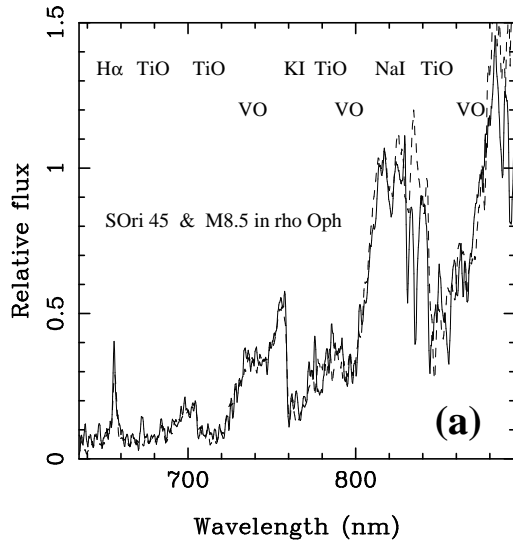


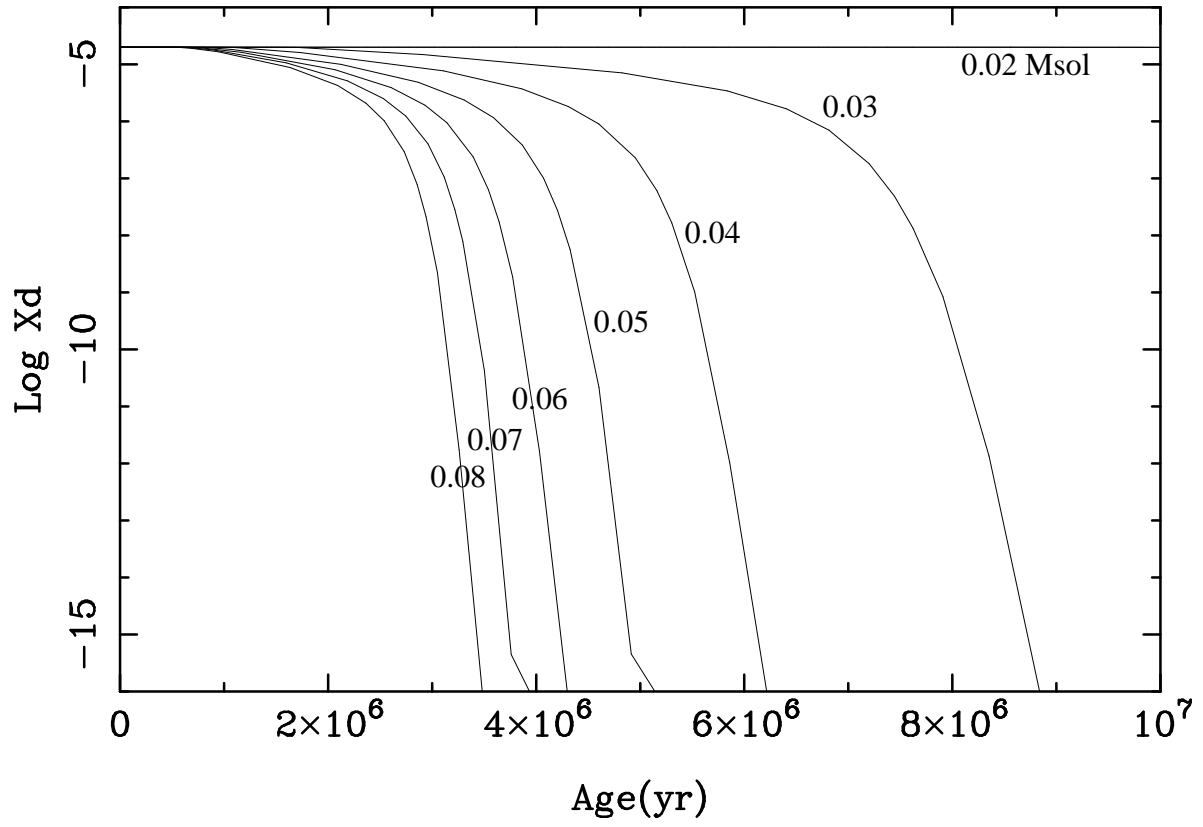


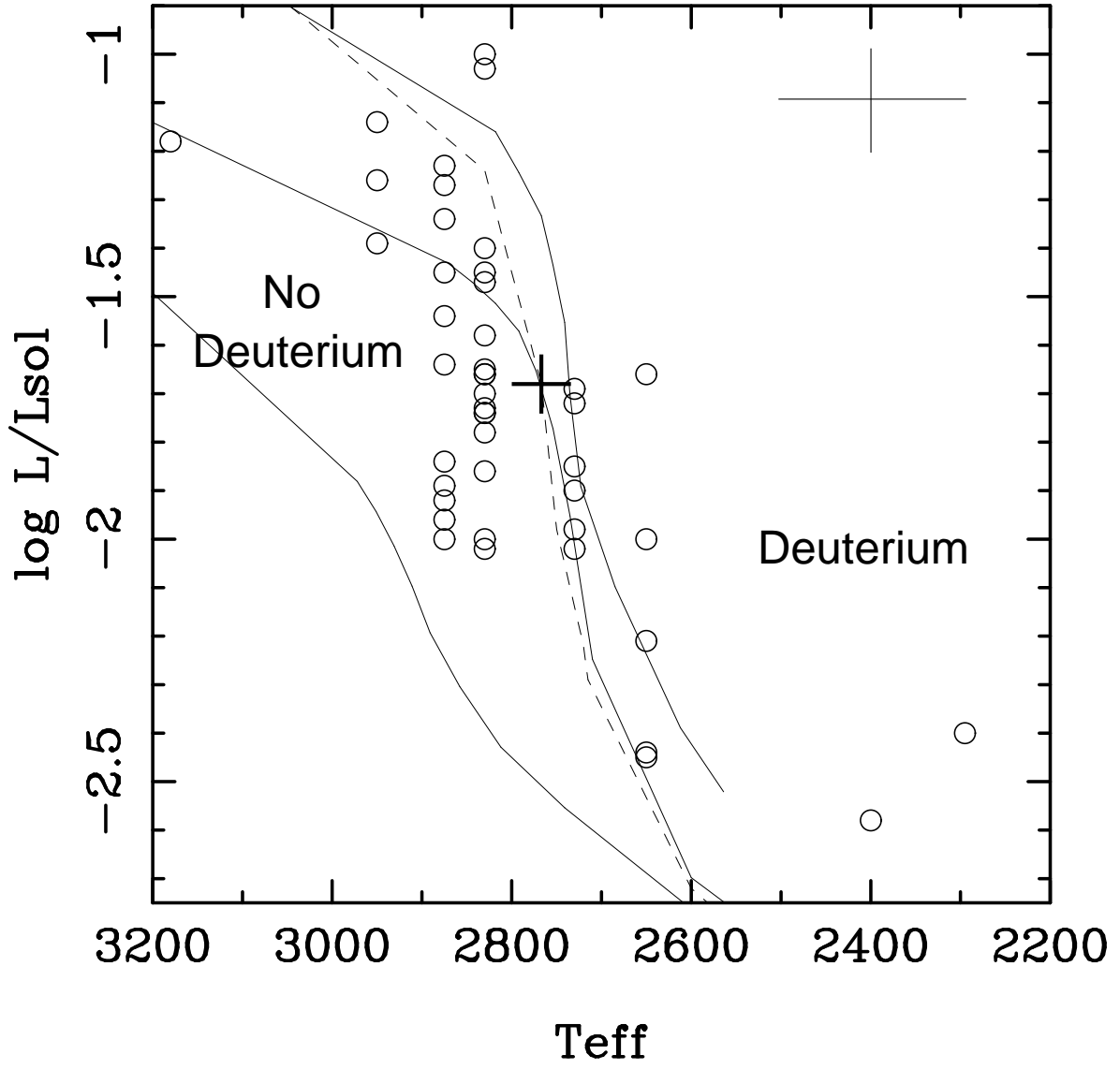












This figure "bejar3a.gif" is available in "gif" format from:

<http://arxiv.org/ps/astro-ph/9903217v1>

This figure "bejar3b.gif" is available in "gif" format from:

<http://arxiv.org/ps/astro-ph/9903217v1>